Bond Graph Aided Performance Analysis of Antilock Braking System for a Bicycle Vehicle Model with Camber Angle and Fork Angle

Dr. Tarun Kumar Bera
Mechanical Engineering Department
Thapar University
Patiala, India
tkbera@thapar.edu

Adityabir Singh
Mechanical Engineering Department
Thapar University
Patiala, India
adityabirsingh@gmail.com

***Abstract*—In most studies, braking of vehicle in a straight path has been considered. When vehicle moves in a curved path, the effect of camber angle and fork angle should be considered. The variable camber angle assists braking in a curved road but the turning radius of vehicle changes due to varying camber angle and fork angle. The antilock braking system (ABS) is used for enhancing vehicle directional stability and steerability. The bond graph model of bicycle vehicle model is developed to study the effect of camber angle and fork angle on the performance of ABS when it maneuvers a curved path.**

Keywords—antilock braking system; bond graph; camber angle; fork angle

I. INTRODUCTION

When brakes are applied to a vehicle with an antilock braking system (ABS), while maneuvering a curved path, the camber angle increases the contact patch of the tyre with the ground up to a certain extent and thus it assists braking. Camber angle can be either positive or negative. When the top of the tyre is tilted outward, it has positive camber angle and when the top of the tyre is tilted inward, it has negative camber angle. A variable camber suspension system (VCSS) having sensor, controller and camber adjuster was developed by Choudhery [**1**]. A suspension system with camber adjustment mechanism while maneuvering a curve, lowers and draws inward the upper A-arm of the outer front tyre, thus provides the negative camber angle [**2**].Two wheelers always has positive camber angle either they are maneuvering left or right turn. Two wheelers require large camber angle and small steering angle while turning.

The vehicle should have small turning radius while maneuvering a curved path. So fork angle should be such that it increases the stability of the vehicle at higher speed and also has small turning radius. If the line drawn through the steering axis meets the road surface slightly ahead of the contact point of the tyre with the ground, it has positive fork angle and if it meets behind the contact point of the tyre with the ground, it has negative fork angle.

Antilock braking system (ABS) maintains the slip ratio in such a range, according to road condition, maximum frictional resistance can be achieved. In this way ABS decreases the braking distance. It uses an on-off control strategy to prevent locking of tyres and thus preventing skidding of vehicle. Thus ABS increases the directional stability and steerability while braking. Friction force between road and tyres during braking is a non-linear function of slip ratio [**3**]. Different ABS controllers have been developed to achieve highest coefficient of friction. The main limitation of conventional ABS is that slip ratio is always maintained in a particular range for any road condition rather than optimal value [**4**]. Bera et al. [**5**] takes into account the load transfer on the wheels while the vehicle maneuvers a curved road and develops an ABS controller which maintain the slip ratio within a desired range. A hardware-in-the-loop (HIL) rig has been developed to investigate slip control for heavy vehicles [**6**]. An ABS controller which uses camber angle and lateral acceleration to control brake pressure was developed by Huang et al. [**7**].

Bond graph represents the paths of exchange of energy within a system structure. Bond graph technique is comparatively easier in modelling of systems consisting of several sub-systems which are residing in different energy domains and formulation of system equations need not be required for bond graph modelling. Bond graph modelling is a unified approach in modelling and simulation of physical systems lying in different energy domains [**8–9**]. One can interpret the energy interactions between different parts of the model and can correct the computational problems by making necessary changes in the model. Bond graph approach is extensively used to study the dynamic response of the vehicle [**10**]. A four wheel model with electrically controlled brakes and steering were developed to study the dynamic response of the vehicle [**11**].

The paper is structured as follows: First relationships between camber angle and fork angle are studied. Then, models of different sub-systems are explained. The bicycle vehicle model is developed with bond graph to study the effect of camber angle and fork angle on the performance of the ABS when it maneuvers a curved path. Finally, parameter values along with simulation results are shown and compared.

Research in this area is supported by University Grants Commission, New Delhi in the framework of Design and Control of Intelligent Autonomous Vehicle (IAV) for Indian Sea Ports.

II. RELATIONSHIPS BETWEEN CAMBER AND FORK ANGLE

Many efforts have been made to increase the coefficient of friction between the tyre and the road while braking. Most important method is by adjusting the camber angle and fork angle of the vehicle. The expression of camber angle (ϕ) as a function of fork angle (λ) and steering angle (δ) is given as [**12**]

$$\cos\phi = \cos\delta \sin^2\lambda + \cos^2\lambda \quad (1)$$

From (1) it is clear that for a fixed steering angle *i.e.* for a fixed turning radius of road, camber angle and fork angle are directly proportional to each other. Since camber angle and fork angle decides the area of contact patch between the tyre and the road, their variation plays an important role in the vehicle stability and steerability specially while maneuvering a curved path. As today roads are very congested with vehicles, small turning radius is desired during lane changing and also during parking. Also, while maneuvering, contact patch of the tyre with the road should be maximized so that braking of the vehicle is efficient. In this paper it will be shown that stopping distance after applying ABS decreases with the increase of positive camber angle and the reverse case happens for the castor angle.

III. MODELLING OF MECHANICAL ANTILOCK BRAKING SYSTEM

Tyres are the points of contact of the vehicle with the road. Rather tyres do not make point contact, they deform due to the vehicle load and make a surface contact called contact patch. All tyre forces and moments are considered to act at the centre of the contact patch of the tyre. The Pacejka's magic formula may be used to calculate the longitudinal force, lateral force and self-aligning moment of the tyres [**13**].

A. Lateral and Longitudinal Tyre Forces

Longitudinal slip ratio of the tyre is an important characteristic to find out whether wheels could be locked during braking. This slip ratio (σ_x) is the ratio of difference between the longitudinal vehicle velocity $(\dot{x})$ and angular velocity $(\dot{\theta}_{ty} r_t)$ of tyre to the linear speed of the vehicle and longitudinal slip ratio during braking is expressed as

$$\sigma_x = \frac{\dot{x} - \dot{\theta}_{ty} r_t}{\dot{x}} \quad (2)$$

Lateral slip ratio (σ_y) is the ratio of lateral velocity $(\dot{y})$ to the longitudinal velocity $(\dot{x})$ of the vehicle and it is given as

$$\sigma_y = \frac{\dot{y}}{\dot{x}} \quad (3)$$

According to the Pacejka's magic formula the force or moment generated (y) can be expressed as a function of input variable (x) as

$$y(x) = D\sin[C\tan^{-1}\{Bx - E(Bx - \tan^{-1}(bx))\}] \quad (4)$$

Where B is stiffness factor, C is shape factor, D is peak value and E is curvature factor and can be determined by measuring tyre forces and moments [**14**]. Output variable (y) can be longitudinal force (F_x), lateral force (F_y) and self-aligning moment(M_z) and input variable (x) can be either longitudinal slip ratio (σ_x) or lateral slip ratio (σ_y). Longitudinal force is generated due to longitudinal slip velocity $(\dot{x} - \dot{\theta}_{ty} r_t)$ and lateral force and self aligning moment are generated due to lateral slip velocity $(\dot{y})$ as there is no initial lateral velocity. The main drawback of Pacejka's magic formula is, it does not take into account the dependence of friction force on the velocity of the vehicle while braking. Though this formula is a good one during motion of the vehicle at constant speed, this model is not used in this present work as velocity decreases during braking.

B. Design of Braking System

Antilock braking system is a dynamic control system which prevents tyres from locking up during braking and provides maximum frictional force by maintaining slip ratio in an optimal range. If the value of slip ratio is high, it means angular velocity of the tyre is decreasing much faster, during braking, as compared to linear velocity of the vehicle. The grip of the tyre with the road is reduced and skidding of the vehicle may occur. Therefore, the brake torque is required to be reduced to increase the angular velocity of the tyre and thus the slip ratio reduces. At low values of slip ratio, the grip between the tyre and road again reduces. Therefore, the brake torque is varied such that slip ratio is maintained in a range bounded by maximum $(\sigma_{\max})$ and minimum $(\sigma_{\min})$ slip values.

The main parts of mechanical equivalent ABS are servo motor, lever arm, brake cable, return spring, brake rod, cam and brake shoe [**4**]. The voltage supply to the servo motor is controlled by ABS controller. One end of the lever arm is connected to the servo motor whereas other is connected to brake rod which rotates the cam. The movement of cam expands and contracts the brake shoe. The return spring is used to come back to the initial position. The schema of ABS is shown in Fig. 1(a).

The calculation of friction force between the tyre and the road is very important in determining the amount of braking torque of the vehicle. Friction model given by Burckhardt is used here to calculate the friction coefficient. It is given as

$$\mu(\sigma_x, \dot{x}_t) = [C_1(1 - e^{-C_2\sigma_x}) - C_3\sigma_x]e^{-C_4\sigma_x\dot{x}_t} \quad (5)$$

Where constant parameter C_1, C_2, C_3 and C_4 are determined experimentally for different road conditions. The values of these parameters for dry asphalt road surface which is very much common in Indian roads are given in TABLE I. Slip-friction curves for different road conditions with a vehicle speed of 10 m/s is shown in [**15**].

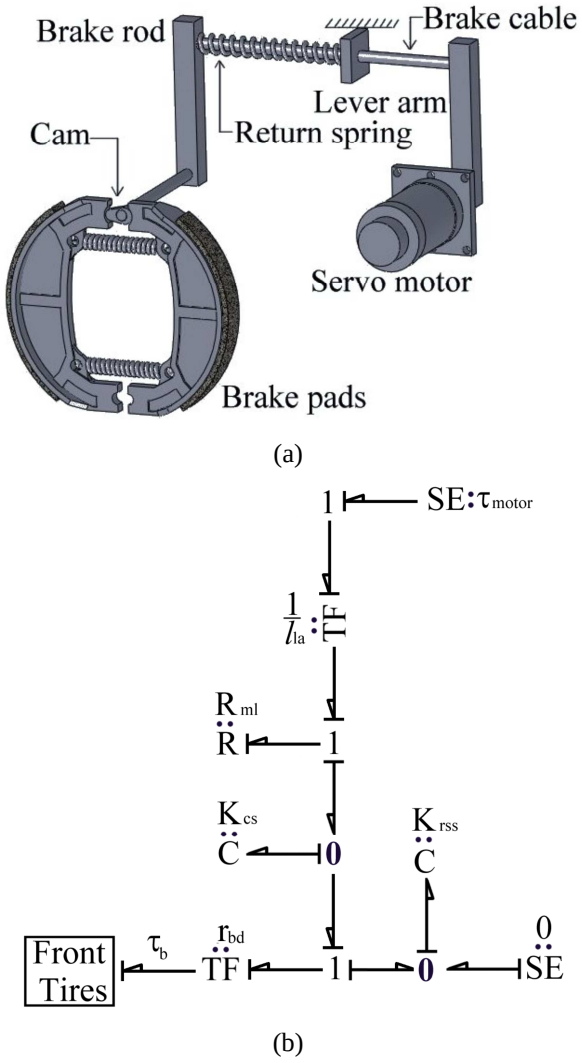

Fig. 1. (a) Schema of mechanical equivalent ABS and (b) its bond graph model [5].

TABLE I. TYRE-ROAD FRICTION PARAMETERS [**3**]

Road Surface	C_1	C_2	C_3	C_4
Asphalt, dry	1.029	17.16	0.523	0.03

The Burckhardt formula takes into account the velocity dependence of frictional force of the vehicle which is very important while designing any braking system. The relation between the braking torque (T) and longitudinal slip ratio (σ) is given below

$$T_{i+1} = \begin{cases} 0 & \sigma > \sigma_{\max} \\ T_i & \sigma_{\min} \le \sigma \le \sigma_{\max} \\ T_{\max} & \sigma < \sigma_{\min} \end{cases} \quad (6)$$

Braking torque should be zero if the value of slip ratio is greater than $\sigma_{\max}$ and maximum braking torque must be applied if slip ratio is less than $\sigma_{\min}$. For all other cases same braking torque is applied as in last step. The optimal range of slip ratio for which maximum frictional force can be obtained is 0.2–0.25 for all kind of road conditions [**5**].

C. Bond Graph of Braking System

The bond graph model of ABS is shown in Fig. 1(b). The controlled amount of voltage from the ABS controller is fed to the motor to produce torque (τ_{motor}) and is represented by the Se element. The mechanical losses are represented by the resistive element (R_{ml}). The cable stiffness (K_{cs}) is represented by the C-element. The return spring stiffness is K_{rss}. The other end of the return spring is connected to zero valued Se element which represents the ground. The output brake torque is applied to the bicycle vehicle model.

IV. BICYCLE VEHICLE MODEL WITH CAMBER AND FORK ANGLE

A bicycle vehicle model is developed to study the effect of roll (ϕ), pitch (λ) and yaw (δ) motions on ABS while maneuvering a curved path. Schematic diagram of bicycle vehicle model is shown in Fig. 2 and its bond graph model is shown in Fig. 3.

A. Kinematic Relations of Bicycle Vehicle Model and its Bond Graph Model

The kinematic relations which are derived in [**5**] have been modified to study the effect of camber angle (ϕ) and fork angle (λ). Major part of the bond graph model of the vehicle has been constructed based on of these relations. Front wheels are steered by an angle (δ). Normal and tangential component of velocity of the front tyres are

$$\left.\begin{aligned} v_{fn} &= (\dot{y} + \dot{\theta}_{cz} a)\cos\delta\cos\phi - \dot{x}\sin\delta\cos\lambda \\ v_{ft} &= (\dot{y} + \dot{\theta}_{cz} a)\sin\delta\cos\phi + \dot{x}\cos\delta\cos\lambda \end{aligned}\right\} \quad (7)$$

Similarly, normal and tangential component of velocity of the rear tyres are

$$\left.\begin{aligned} v_{rn} &= (\dot{y} - \dot{\theta}_{cz} b)\cos\phi \\ v_{rt} &= \dot{x} \end{aligned}\right\} \quad (8)$$

Newton-Euler equations based on external forces, inertial forces and gyroscopic forces are given by

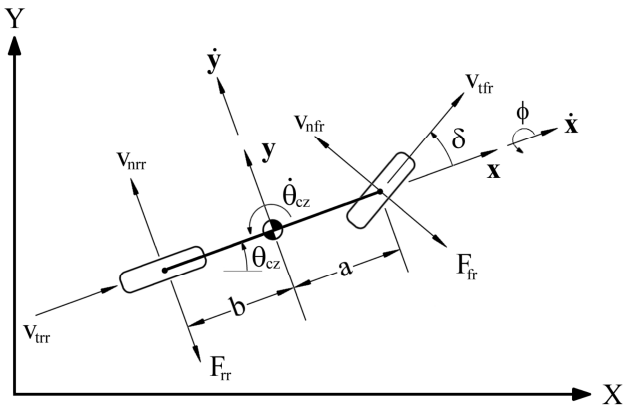

Fig. 2. Schema of bicycle vehicle model.

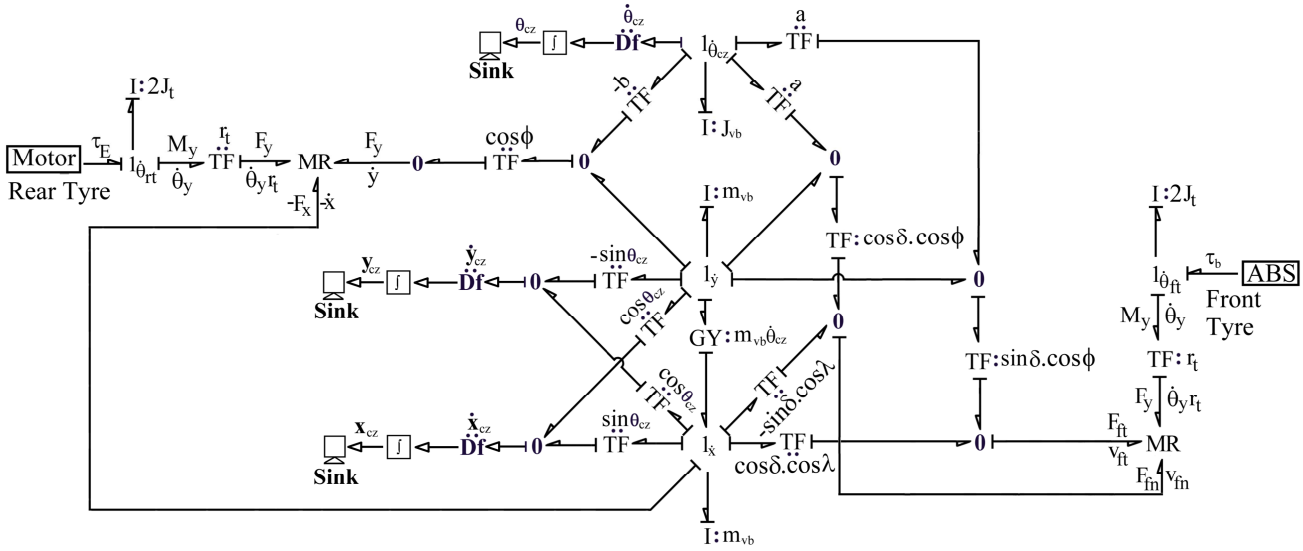

Fig. 3. Bond graph of bicycle vehicle model.

$$\left.\begin{aligned} m_{vb}\ddot{x} &= m_{vb}\dot{\theta}_{cz}\dot{y} + \sum F_x \\ m_{vb}\ddot{y} &= -m_{vb}\dot{\theta}_{cz}\dot{x} + \sum F_y \end{aligned}\right\} \tag{9}$$

The bond graph of bicycle vehicle model has been constructed using (7–9) and is shown in Fig. 3. Torque from the electric traction motor (τ_E) is applied to the rear tyres whereas the braking torque (τ_B) from the ABS unit is applied to the front tyres. Power bonds are represented by half arrows, whereas information bonds are represented by full arrow. Vehicle inertial mass $(I : m_{vb})$ and rotary inertia $(I : J_{vb})$ is modeled at their respective 1-junctions which represent the linear and angular velocity of the centroid of the vehicle in the body fixed coordinate system.

The two modulated 3-port R-field (MR-elements) implement the Burckhardt formula. Tangential and normal components of the velocity are used to calculate the slip ratio by using (2–3). Therefore Burckhardt formula (5) is used to calculate the coefficient of friction and hence to calculate the longitudinal and lateral tyre forces.

V. Parameter Values and Simulation Results

The parameter values used in the simulation is given in Table 2. The value of the constant parameters used in Burckhardt formula is taken from Table 1. The control logic based on (6) adjust the brake torque such that slip ratio always lies between 0.2–0.25. The road is considered as made of dry asphalt. The radius of the wheel is 0.3 m. The length of the vehicle is 2 m.

All simulations are performed in SYMBOLS Shakti software [**16**]. It is an object oriented modelling and simulation technique which allows users to create models using bond graph. It automatically derives the reduced system equations from the bond graph model. The software has number of in-built as well as user made capsules of different basic engineering components. High level control analysis can also be performed using this software.

TABLE II. Parameter Values of Bicycle Vehicle Model

Subsystem	Parameter Values			
Vehicle body	$m_{vb} = 1000$ kg	$J_{vb} = 100$ kg m^2	$a = 1.0$ m	$b = 1.0$ m
Wheel	$r_t = 0.3$ m	$J_t = 100$ kg m^2		
	$C_1 = 1.029$	$C_2 = 17.16$	$C_3 = 0.523$	$C_4 = 0.03$
ABS	$\sigma_{max} = 0.25$	$\sigma_{min} = 0.2$		
Motor	$V = 100$ V	$\mu = 0.4$ Nm/A	$R = 0.1\,\Omega$	$G = 8$

First, bond graph of the bicycle model is made in the bond pad and then simulation is done in symbols simulator. The parameters are properly considered and put in the simulator from Table I and Table II. Then simulation is done for different values of the camber and fork angle. The practical range of camber angle (ϕ) is 0.2–0.5 rad. and that of fork angle (λ) is 0.3–0.8 rad. The value of steering angle (δ) is kept fix to 0.1 rad. and is applied at t = 10 s. ABS is applied to the front wheels of the bicycle model whereas rear wheels are motor driven.

A. *Effect of Camber Angle Without Antilock Braking System*

Fig. 4(a) shows the variation of camber angle and for no fork angle while maneuvering a curved path. It shows that the path traversed by the vehicle without camber angle which is a circle of diameter 52.22 m (base diameter). The diameter of the path is reduced by 61.35 cm if the camber angle of 0.2 rad. is considered and the path is reduced by 143.84 cm (with respect to base diameter) if the camber angle is 0.3 rad. Also, there is decrease in the longitudinal speed of 0.43 mm/s for 0.2 rad. and 1.03 mm/s for 0.3 rad. (which is shown in Fig. 4(b)) with respect to the speed of 10.81528 m/s which is the speed of the vehicle for without any camber angle. It is also observed from the Fig. 4(b) that the speed of the vehicle reduces due to the starting of the yaw motion of the vehicle at 10 s.

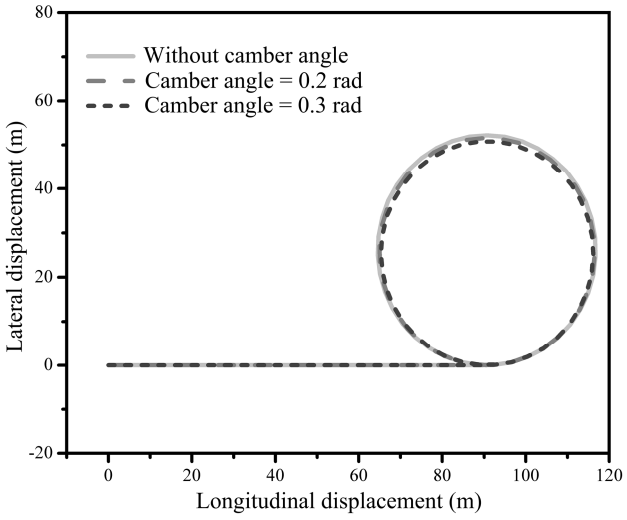

(a)

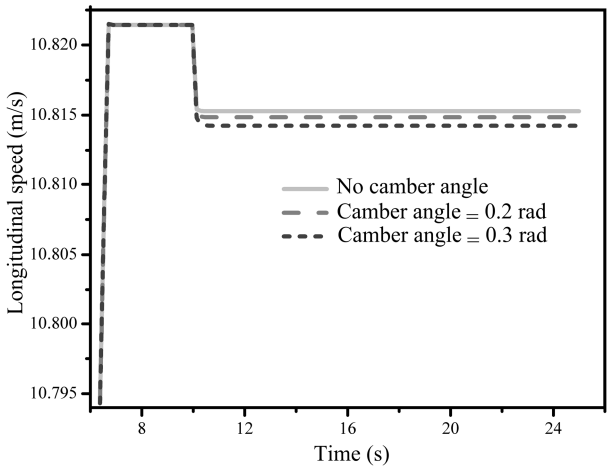

(b)

Fig. 4. (a) Lateral vs. longitudinal displacement of the centre of vehicle for different camber angles while maneuvering a curved path and (b) corresponding longitudinal speeds with no fork angle.

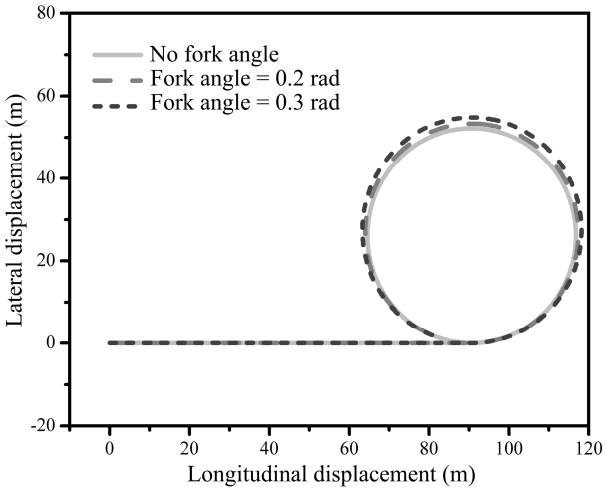

(a)

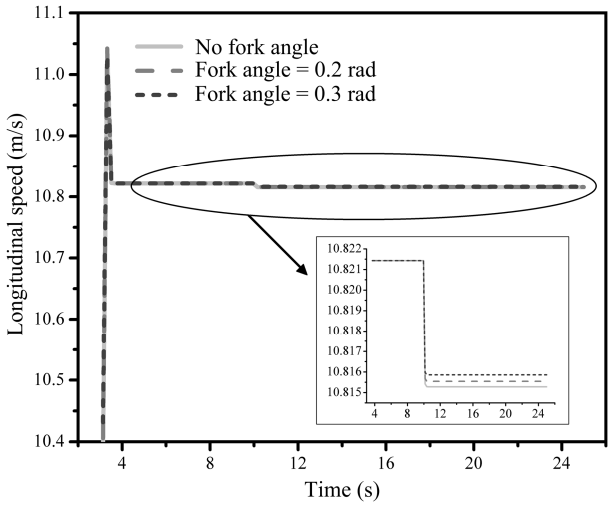

(b)

Fig. 5. (a) Lateral displacement vs. longitudinal displacement of the centre of vehicle for different fork angles while maneuvering a curved path and (b) corresponding longitudinal speeds with no camber angle.

B. Effect of Fork Angle Without Antilock Braking System

Fig. 5(a) shows that the path (thick grey line) traversed by the vehicle without fork angle is a circle of diameter 52.22 m (No camber and fork angle is provided to the wheel). The diameter of the circle is increased by 115.12 cm if the fork angle of wheel is 0.2 rad. and the path is increased by 264.4 cm with respect to the base diameter if the fork angle is 0.3 rad. Also, the longitudinal speed is increased by 0.26 mm/s for 0.2 rad. and increased by 0.58 mm/s for 0.3 rad. (Fig 5(b)) with respect to the base speed of 10.81528 m/s.

C. Effect of Camber and Fork Angle on Turning Radius without Antilock Braking System

Fig. 6(a) shows the effect of camber angle on turning radius for different values of fork angle. It clearly shows that turning radius always decreases if we increase the camber angle. So camber angle is inversely proportional to the turning radius. Similarly, Fig. 6(b) shows the effect of fork angle on turning radius for different values of the camber angle. The turning radius always increases if we increase the fork angle. For fixed turning radius, camber angle is proportional to fork angle as proposed in [**12**].

D. Effect of Camber and Fork Angle Individually on Antilock Braking System

The effect of camber angle and fork angle on ABS is shown in Fig. 7. Initially the vehicle starts from rest and then it reaches at a speed of 33.6 km/hr at 8 s. At 10 s the vehicle is steered with a steering angle of 0.1 rad and the ABS is applied at 15 s to stop the vehicle. It takes 1.5 s after applying the brake to stop the vehicle. It is seen from Fig. 7(a), the vehicle exactly follows the path when ABS is applied with no camber angle. Fig 7(a) shows that, the stopping distance and turning radius both decrease with an increase in camber angle. So, increase in camber angle is advantageous during braking but it can not be increased after the specific limit (maximum limit of camber angle is 0.5 rad) as the path of contact between the tyre and the road again starts decreasing after that specific limit. The increase in fork angle decreases the stopping distance but it increases the turning radius while maneuvering a curved

path (Fig. 7(b)) but fork angle must be provided to the wheel to enhance the stability of the vehicle.

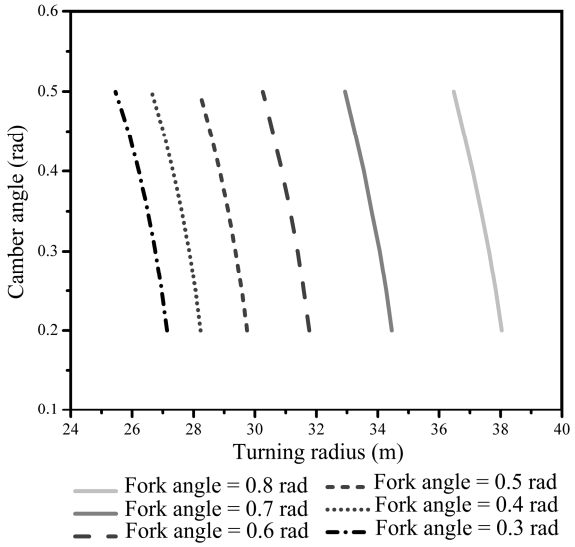

(a)

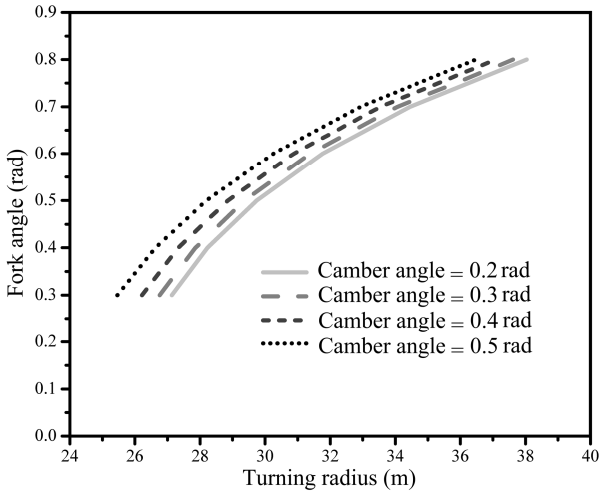

(b)

Fig.6. Variation of (a) camber angle with turning radius for different values of fork angle and (b) castor angle with turning radius for different values of camber angle.

E. Effect of Camber and Fork Angle for a Fixed Value of the Other on Antilock Braking System

Fig. 8(a) shows the effect of camber angle while ABS is applied to the vehicle maneuvering a curved path for a fixed value of fork angle of 0.3 rad. The effect of fork angle while ABS is applied to the vehicle maneuvering a curved path for fixed value of camber angle 0.2 rad is shown in Fig. 8(b). It is concluded from Fig. 8, if the camber angle of 0.2 rad and fork angle of 0.3 rad is provided to the wheel, both stability of the vehicle can be enhanced as well as the vehicle follows the road. The slip ratio is maintained between 0.2 and 0.25 to obtain the maximum frictional force between the wheel and road and it is shown in Fig. 9(a). In Fig. 9(b), the vehicle speed and the corresponding speed of front wheel on which ABS is attached are shown. The angular speed of the front wheel is shown in inset during braking.

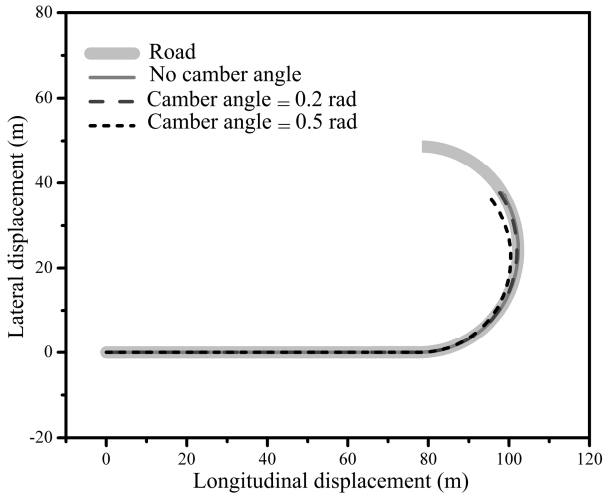

(a)

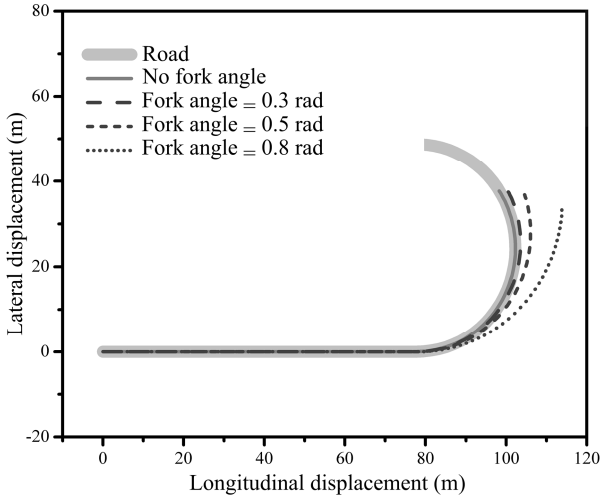

(b)

Fig.7. Lateral vs. longitudinal displacement of the centre of vehicle for different (a) camber angles with no fork angle and (b) castor angles with no camber angle.

VI. CONCLUSIONS

Bond graph of bicycle vehicle model has been developed to observe the effect of camber angle and fork angle on ABS while maneuvering a curved path. It has been concluded that camber angle decreases the stopping distance as well as turning radius of the vehicle. On the other hand, fork angle increases the turning radius of the vehicle. Increase in camber angle reduces the longitudinal speed of the vehicle while turning. But increase in fork angle increases the longitudinal speed of the vehicle. For a fixed value of turning radius, if we increase the castor angle, camber angle will also increases.

REFERENCES

[1] K.H. Choudhery, "Variable camber suspension system," United States Patent, US 6,874,793 B2, 2005.

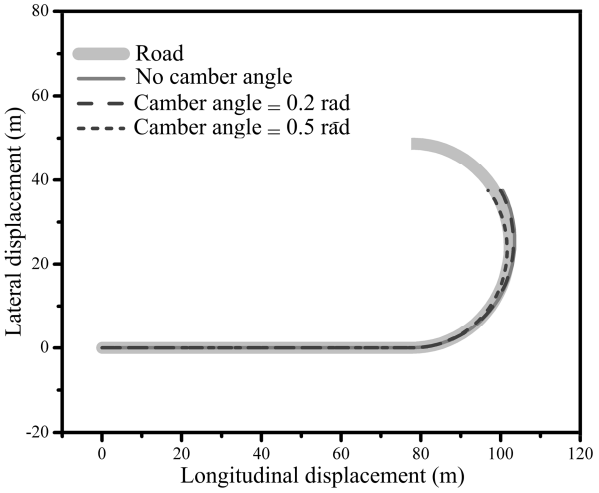

(a)

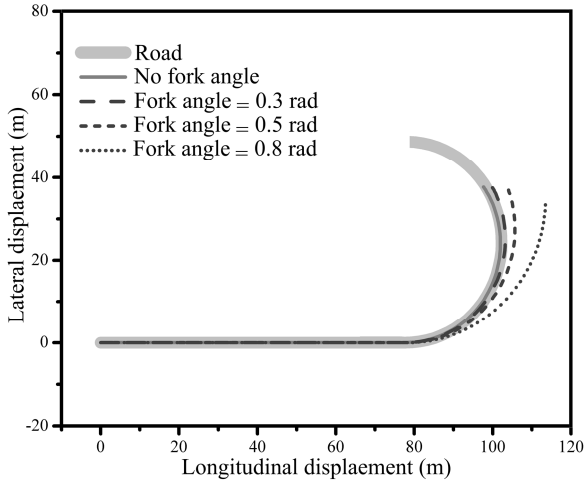

(b)

Fig.8. Lateral vs. longitudinal displacement of centre of vehicle for different (a) camber angles with 0.3 rad fork angle and (b) castor angles with 0.2 rad camber angle.

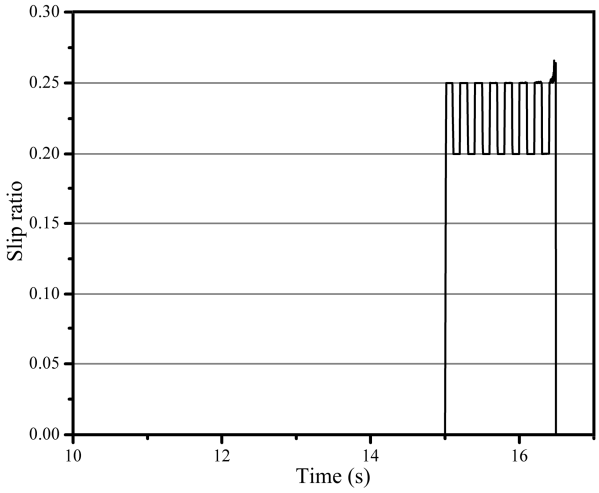

(a)

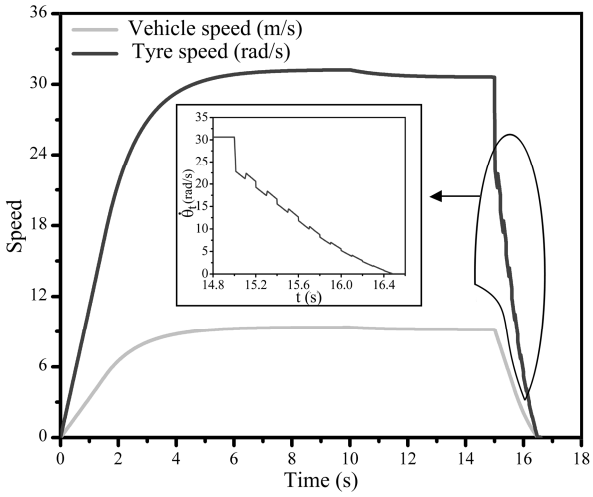

(b)

Fig.9. (a) Slip ratio vs. time and (b) vehicle and wheel speed vs. time.

[2] R. Boston, "Vehicle suspension system with a variable camber system," United States Patent, US 7,914,020 B2.

[3] M. Oudghiri, M. Chadli, and A.E. Hajjaji, "Robust fuzzy sliding mode control for antilock braking system," International Journal on Sciences and Techniques of Automatic Control, vol. 1, pp. 13-28, 2007.

[4] R.G. Longoria, A. Al-Sharif, and C.B. Patil, "Scaled vehicle system dynamics and control: a case study in anti-lock braking," International Journal of Vehicle Autonomous Systems, vol. 2, pp. 18-39, 2004.

[5] T.K. Bera, K. Bhattacharya, and A.K. Samantaray, "Evaluation of antilock braking system with an integrated model of full vehicle system dynamics," Simulation Modeling Practice and Theory, vol. 19, pp. 2131-2150, 2011.

[6] F.W. Kienhofer, J.I. Miller, and D. Cebon, "Design concept for an alternative heavy vehicle ABS system," Vehicle System Dynamics, vol. 46, pp. 571-583, 2008.

[7] C.K. Huang and M.C. Shih, "Dynamic analysis and control of an antilock brake system for a motorcycle with a camber angle," Vehicle System Dynamics, vol. 49, pp. 639-656, 2011.

[8] D.C. Karnopp, D.L. Margolis, and R.C. Rosenberg, System Dynamics, Modeling and Simulation of Mechatronic Systems. John Wiley & Sons, NY, 2000.

[9] A. Mukherjee, R. Karmakar, and A.K. Samantaray, Bond Graph in Modeling, Simulation and fault Identification. CRC Press, FL, 2006.

[10] D. Hrovat, J. Asgari, and M. Fodor, Automotive Mechatronic Systems. In: Mechatronic Systems Techniques and Applications, Gordon and Breach Science Publishers, Amsterdam, 2000, pp. 1-98.

[11] H.B. Pacejka, "Modelling complex vehicle systems using bond graphs," Journal of the Franklin Institute, vol. 319, pp. 67-81, 1985.

[12] R.N. Jazar, A. Subic, and N. Zhang, "Kinematics of a smart variable caster mechanism for a vehicle steerable wheel," Vehicle System Dynamics, vol. 50, pp. 1861-1875, 2012.

[13] H.B. Pacejka, Tyre and Vehicle Dynamics. Butterworth-Heinemann, Elsevier, UK, 2006.

[14] R. Rajamani, Vehicle Dynamics and Control. Springer, US, 2006.

[15] T.K. Bera, K. Bhattacharya, and A.K. Samantaray, "Bond graph model based evaluation of a sliding mode controller for combined regenerative and antilock braking system," Proceedings of the Institution of Mechanical Engineers, Part I: Journal of Systems and Control Engineering, vol. 225, pp. 918-934, 2011.

[16] SYMBOLS User's Manual, High Tech Consultants. <http://www.htcinfo.com>.